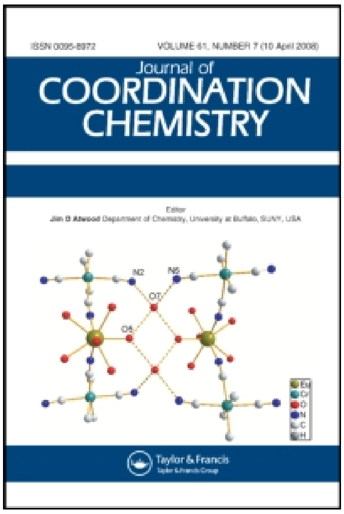

Journal of Coordination Chemistry
Publication details, including instructions for authors and subscription information:
http://www.informaworld.com/smpp/title~content=t713455674

Mixed ligand complexes of β-diketonates: synthesis, characterization, and FAB mass spectral analysis

Ram Lakhan Prasad[a]; Anita Kushwaha[a]; Bhanu Pratap S. Gautam[a]
[a] Faculty of Science, Department of Chemistry, Banaras Hindu University, Varanasi-221005, India

To cite this Article Prasad, Ram Lakhan , Kushwaha, Anita and Gautam, Bhanu Pratap S.(2009) 'Mixed ligand complexes of β-diketonates: synthesis, characterization, and FAB mass spectral analysis', Journal of Coordination Chemistry, 62: 18, 2983 — 2994

To link to this Article: DOI: 10.1080/00958970902954102

URL: http://dx.doi.org/10.1080/00958970902954102

Journal of Coordination Chemistry
Vol. 62, No. 18, 20 September 2009, 2983–2994

Taylor & Francis
Taylor & Francis Group

Mixed ligand complexes of β-diketonates: synthesis, characterization, and FAB mass spectral analysis

RAM LAKHAN PRASAD*, ANITA KUSHWAHA and
BHANU PRATAP S. GAUTAM

Faculty of Science, Department of Chemistry, Banaras Hindu University,
Varanasi – 221005, India

(*Received 14 November 2008; in final form 23 January 2009*)

Complexes of the type $MLL' \cdot nB$ (where $M = Ni(II)$ and $Cu(II)$; LH and $L'H = 2,4$-pentanedione (acacH), 1-phenyl-1,3-butanedione (bacH), and 1,3-diphenyl-1,3-propanedione (dbmH); $n = 0$ to 2 and $B =$ water or pyridine) have been synthesized and characterized. IR spectra are consistent with uninegative bidentate ligands. Magnetic moments and electronic spectral studies reveal high-spin octahedral geometry for nickel(II) complexes and distorted octahedral stereochemistry for copper(II) complexes. Frozen chloroform solution ESR spectra of the copper(II) complexes display significant Jahn–Teller distortion and dimeric behavior of the complexes in solution. FAB mass spectra of the copper(II) complexes also exhibit peaks corresponding to dimers. Molecular, pseudo-molecular, dimeric pseudo-molecular, and fragment ion peaks in unit resolution mass spectra have been identified with the help of their isotope distribution pattern expected due to natural abundances of the ^{63}Cu and ^{65}Cu isotopes. All the FAB mass spectral peaks from the fragment ions containing copper have been interpreted on the basis of isotope distribution pattern.

Keywords: β-diketonates; Mixed ligand complexes; FAB mass spectra of β-diketonates; ESR spectra of mixed ligand complexes

1. Introduction

Metal β-diketonates are versatile compounds used in cancer treatment [1] and as catalysts in polymerization reactions [2–4]. Metal β-diketonates have also been used as precursors for metal–organic chemical vapor deposition (MOCVD) for preparation of high Tc superconducting oxides [5–8]. The synthesis and characterization of binary metal(II) β-diketonates have been extensively studied [1–11]. However, reports on mixed ligand complexes of β-diketonates are limited [12–15]. The mixed ligand complexes play important roles in biological systems [1, 16, 17], catalysis [2, 9, 18] as reaction intermediates [19] and in redox reactions [20]. Meléndez [1] reported that *bis*(β-diketonato)dialkoxytitanium(IV) is an anticancer agent and proposed that this

---

*Corresponding author. Email: rlp@bhu.ac.in; rlpjc@yahoo.co.in

ISSN 0095-8972 print/ISSN 1029-0389 online © 2009 Taylor & Francis
DOI: 10.1080/00958970902954102

complex binds with macromolecules like DNA through coordinate bonds. Interaction of metal β-diketonates with DNA leads to formation of mixed ligand complexes which are labile during their actions in biological systems. Nizel'skii *et al.* [9] have shown that copper β-diketonates are catalysts in the formation of polyurethane from 4,4′-diphenylmethane diisocyanate and diethylene glycol in a process of catalyst complexation with diethylene glycol. The catalytic activity of the catalysts is related to electronic structures and basicities of the β-diketones. It is thus important to study mixed ligand complexes, where two different ligands have different basicities and charge densities are expected to vary on various coordinated β-diketones as compared to *bis* binary complexes. In the present communication, we report synthesis of nickel(II) and copper(II) mixed ligand complexes of β-diketonates [acac$^-$ = 2,4-pentanedionato(acetylacetonato), bac$^-$ = 1-pheny-1,3-butanedionato(benzoylacetonato), and dbm$^-$ = 1,3-diphenyl-1,3-propanedionato(dibenzoylmethanato)] and their characterization using elemental analysis, IR, UV, ESR, and FAB mass spectral studies. *Bis*-binary copper β-diketonates, which are axially symmetric, have been reported to be dimers from ESR spectral studies [21, 22]. The axial symmetry disappears on mixed ligand complex formation and, therefore, it is of interest to study the behavior of mixed ligand complexes toward dimerization after lowering the symmetry of the complexes. Previous workers have interpreted degradation pathways for *bis*-binary metal β-diketonates from their EI mass spectra. However, they have not discussed the isotope distribution pattern of molecular and fragment ions containing copper atoms [23–26] except a few [6, 27], where some of the m/z ion peaks have been shown to exhibit isotope distribution pattern. In this article we interpret all the FAB mass spectral peaks of ternary copper(II) complexes with the help of ^{63}Cu and ^{65}Cu isotope contributions. Molecular/fragment ion ($[\mathrm{m}]^+$) peaks which are not accompanied by corresponding $[m+2]^+$ ion peaks, i.e., peak contributed by ^{65}Cu have been discarded assuming that they arise due to contribution of matrix, ligand, and/or their combinations.

2. Experimental

All chemicals used in the present study were of analytical reagent grade. Metal acetylacetonates were prepared by methods described in [28].

2.1. *Preparation of heterochelate complexes*

2.1.1. *In situ* method. Ternary complexes Ni(acac)(bac)$\cdot 2H_2O$ and Cu(acac)(bac) were synthesized by adding dropwise an aqueous solution (15 mL) of metal chloride (5 mmol) to a mixture of acetylacetone (0.50 g, 5 mmol), benzoylacetone (0.81 g, 5 mmol), and potassium hydroxide (0.56 g, 10 mmol) in 25 mL of a solvent mixture containing 10% acetone, 70% ethanol, and 20% distilled water with constant stirring for 30 min. The resulting precipitates were filtered, washed with ethanol, and dried *in vacuo*.

Ni(acac)(bac)$\cdot 2H_2O$: yield 1.24 g (70%); color: green; m.p.: 149°C.
Cu(acac)(bac): yield 1.21 g (75%); color: blue; decomposition temperature: 160°C.

Preparation of Cu(acac)(dbm). Cu(acac)(dbm) was prepared by the method described earlier using the following solvent mixture (30 mL): 25% acetone, 50% ethanol, and 25% water. Yield 1.64 g (85%), color: blue, decomposition temperature is 195°C.

Preparation of Cu(bac)(dbm) and Ni(bac)(dbm) $\cdot$ *$2H_2O$.* These complexes were also prepared by the above method using a solvent mixture (35 mL) of 50% acetone, 40% ethanol, and 10% distilled water.

Cu(bac)(dbm): yield 2.01 g (90%); color: blue; decomposition temperature: 210°C.
Ni(bac)(dbm) $\cdot$ $2H_2O$: yield 2.10 g (88%); color: yellowish green; m.p.: 190°C.

2.1.2. Substitution method. *Preparation of Cu(acac)(bac), Cu(acac)(dbm), and Ni(acac)(bac)* $\cdot$ *$2H_2O$.* A solution of potassium hydroxide (0.28 g, 5 mmol) and benzoylacetone (0.81 g, 5 mmol) or dibenzoylmethane (1.12 g, 5 mmol) in 25 mL of 60% acetone, 20% ethanol, and 20% distilled water was added dropwise to a solution of $M(acac)_2$ (5 mmol) in 125 mL ethanol with constant stirring for 1 h. The heterochelate complexes that precipitated were filtered, washed with ethanol, and dried *in vacuo*.

Preparation of pyridine adduct. Excess pyridine (1.6 g, 20 mmol) was added to an ethanolic (20 mL) suspension of the ternary complexes (5 mmol). The reaction mixture was stirred for 0.5 h. Excess solvent was evaporated and addition of diethyl ether (20 mL) to the residue resulted in precipitation of the adduct which was filtered, washed with diethyl ether, and dried in air.

2.2. *Analyses and measurements*

Carbon and hydrogen were determined microanalytically. Water content of the complexes was determined by heating them in the range 100–120°C and observing the weight losses [14, 15, 29]. Positive ion FAB mass spectra were recorded on a Jeol SX 102/DA-6000 mass spectrometer at room temperature using *m*-nitrobenzyl alcohol (NBA) as matrix. IR spectral and other physico-chemical measurements were made as described earlier [13, 30].

3. Results and discussion

3.1. *Synthesis and characterization*

Ni(acac)(bac) $\cdot$ $2H_2O$, Ni(bac)(dbm) $\cdot$ $2H_2O$, Cu(acac)(bac), Cu(acac)(dbm), and Cu(bac)(dbm) were prepared by the *in-situ* method as shown,

$$\mathrm{AcacH} + \mathrm{bacH} + 2\mathrm{NaOH(aq)} + \mathrm{MCl_2} \longrightarrow \mathrm{M(acac)(bac)} + 2\mathrm{NaCl} + 2\mathrm{H_2O}$$

Cu(acac)(bac), Cu(acac)(dbm), and Ni(acac)(bac) $\cdot$ $2H_2O$ were prepared by the substitution method, represented as,

$$\mathrm{M(acac)_2} + \mathrm{bac^{-}Na} + \longrightarrow \mathrm{M(acac)(bac)} + \mathrm{acac^{-}Na^{+}}$$

Cu(acac)(bac), Cu(acac)(dbm), and Ni(acac)(bac) $\cdot$ $2H_2O$ were prepared by both the methods. Their analyses exhibit identical results and physico-chemical properties; however, an attempt to synthesize Ni(acac)(dbm) failed by both the methods, resulting in formation of $Ni(dbm)_2$.

Elemental analyses (table 1) are consistent with the stoichiometry MLL′ for the copper(II) and MLL′ · 2B for the nickel(II) complexes [L and L′ = acac⁻, bac⁻, or dbm⁻; B = water or pyridine]. TLC of Ni(acac)(bac) · $2H_2O$, $Ni(acac)_2 \cdot 2H_2O$, and $Ni(bac)_2 \cdot 2H_2O$ recorded in 60% ethanol, 20% DMF, and 20% water yielded a single spot with R_f values of 0.79, 0.86, and 0.74, respectively. These data indicate that Ni(acac)(bac) · $2H_2O$ is a new species and not a mixture of $Ni(acac)_2 \cdot 2H_2O$ and $Ni(bac)_2 \cdot 2H_2O$. Similarly, Ni(bac)(dbm) · $2H_2O$, $Ni(bac)_2 \cdot 2H_2O$, and $Ni(dbm)_2$ yielded a single spot with R_f values of 0.71, 0.79, and 0.61, respectively, suggesting that Ni(bac)(dbm) · $2H_2O$ is also a new species. Further, when chromatograms of equimolar mixture of $Ni(acac)_2 \cdot 2H_2O + Ni(bac)_2 \cdot 2H_2O$ and $Ni(bac)_2 \cdot 2H_2O + Ni(dbm)_2$ were recorded, a single spot was obtained in each case with R_f values same as mentioned earlier for Ni(acac)(bac) · $2H_2O$ and Ni(bac)(dbm) · $2H_2O$, respectively, suggesting formation of ternary complexes, presumably due to rapid and complete redistribution of two *β*-diketonate moieties as a consequence of greater stability of the ternary complex as compared to their *bis*-binary complexes.

$$\mathrm{Ni(acac)_2 \cdot 2H_2O + Ni(bac)_2 \cdot 2H_2O \xrightarrow{80\%\ \text{ethanol and}\ 20\%\ \text{DMF}} 2Ni(acac)(bac) \cdot 2H_2O}$$

Hydrated ternary complexes yielded anhydrous complexes on heating in the range 100–120°C for 2 h. The complexes are either sharply melting solids or decompose above 160°C, are insoluble in water, slightly soluble in organic solvents (ethanol, methanol, benzene, chloroform, etc.) but highly soluble in highly polar solvents like DMF, DMSO, etc. The molar conductance of the complexes in DMF lie in the range 1.79–3.15 $\mathrm{Ohm^{-1}\,cm^2\,mol^{-1}}$ indicating non-electrolytes [31].

Table 1. Analytical data of the heterochelate complexes.

Complex	Empirical formula (formula weight)	Found (Calcd)% C	H	Water loss	Magnetic moment (B.M.)	Molar conductance ($\mathrm{Ohm^{-1}\,cm^2\,mol^{-1}}$)
Ni(acac)(bac) · $2H_2O$	$C_{15}H_{20}NiO_6$ (355.02)	51.05 (50.75)	5.60 (5.68)	10.56 (10.15)	3.09	3.09
Ni(bac)(dbm) · $2H_2O$	$C_{25}H_{24}NiO_6$ (479.16)	63.14 (62.67)	5.25 (5.05)	7.20 (7.52)	3.10	3.15
Ni(acac)(bac)	$C_{15}H_{16}NiO_4$ (318.99)	55.95 (56.48)	5.15 (5.06)	–	3.05	2.95
Ni(bac)(dbm)	$C_{25}H_{20}NiO_4$ (443.13)	67.45 (67.76)	4.25 (4.55)	–	3.03	3.05
Ni(acac)(bac) · 2py	$C_{25}H_{26}N_2NiO_4$ (477.19)	–	–	–	3.03	2.95
Ni(bac)(dbm) · 2py	$C_{35}H_{30}N_2NiO_4$ (601.34)	–	–	–	2.97	2.97
Cu(acac)(bac)	$C_{15}H_{16}CuO_4$ (323.84)	55.84 (55.63)	4.88 (4.98)		1.74	1.85
Cu(bac)(dbm)	$C_{25}H_{20}CuO_4$ (447.98)	66.82 (67.03)	4.81 (4.50)		1.75	1.82
Cu(acac)(dbm)	$C_{20}H_{18}CuO_4$ (385.91)	62.56 (62.25)	4.27 (4.70)		1.72	2.34

3.2. *IR spectra*

The IR spectra of the hydrated nickel(II) ternary complexes exhibit a broad band in the region 3200–3600 cm^{-1} due to ν(O–H) and at 850 cm^{-1} due to the bending mode of the O–H. Presence of the latter band indicates coordination of water. These bands are absent in the spectra of anhydrous nickel(II) complexes, their pyridine adducts and copper(II) complexes. Spectra of pyridine adducts show bands at ~1060, ~630, and ~460 cm^{-1}, assigned to the ring breathing, in-plane, and out-of-plane bending vibrations, respectively, characteristics of coordinated pyridine [32, 33].

The spectrum of Cu(acac)$_2$ has absorption bands due to $\nu(\mathrm{C}\underline{\cdots}\mathrm{O})$, $\nu(\mathrm{C}\underline{\cdots}\mathrm{C})$, δ(C–H), and ω(C–CH$_3$) at 1570, 1520, 1188, and 1265 cm^{-1}, respectively, while that of Cu(bac)$_2$ shows these bands at 1585, 1520, 1210, and 1275 cm^{-1}, respectively, with an additional band at 1300 cm^{-1} ascribed to the ω(C–Ph) vibration [6, 27]. In the spectra of ternary complexes the $\nu(\mathrm{C}\underline{\cdots}\mathrm{O})$, $\nu(\mathrm{C}\underline{\cdots}\mathrm{C})$, δ(C–H), and ω(C–R) (R = CH$_3$ or Ph) absorptions are observed as broader bands with respect to those of corresponding bands in their *bis*-binary complexes in the regions 1575–1600, 1510–1535, 1190—1220, and 1260–1305 cm^{-1}, respectively, characteristic of uninegative bidentate β-diketonates [32–34].

3.3. *Magnetic moments*

Magnetic moments of the nickel(II) complexes were in the range 2.97–3.10 μ_B consistent with the high-spin octahedral nickel(II) complexes. The μ_eff values of all the copper(II) complexes are in the range 1.70–1.74 μ_B as expected for one unpaired electron [35, 36].

3.4. *Electronic spectra*

Electronic spectra of Ni(acac)(bac) · 2H$_2$O, Ni(acac)(bac), Ni(bac)(dbm) · 2H$_2$O, and Ni(acac)(bac) · 2py exhibit two d–d transitions in the range 9300–10,000 and 15,100–16,000 cm^{-1} attributed to $^3\mathrm{T}_{2\mathrm{g}}(\mathrm{F}) \leftarrow {}^3\mathrm{A}_{2\mathrm{g}}(\mathrm{F})$ (ν_1) and $^3\mathrm{T}_{1\mathrm{g}}(\mathrm{F}) \leftarrow {}^3\mathrm{A}_{2\mathrm{g}}(\mathrm{F})$ (ν_2), respectively, on the basis of octahedral geometry. The spectrum of Ni(bac)(dbm) · 2py, besides showing ν_1 and ν_2 bands in the above mentioned ranges, exhibits an additional band at 25,000 cm^{-1} due to $^3\mathrm{T}_{1\mathrm{g}}(\mathrm{P}) \leftarrow {}^3\mathrm{A}_{2\mathrm{g}}(\mathrm{F})$ (ν_3). The spectrum of the anhydrous complex Ni(bac)(dbm) yields ν_1 and ν_3 bands at 9320 and 23,530 cm^{-1}, respectively, suggesting an octahedral stereochemistry of the complex [36, 37].

In the spectrum of Cu(bac)(dbm), three d–d transition bands are observed at 15,750, 18,690, and 22,990 cm^{-1} assigned to the transitions $\mathrm{d}_{x^2-y^2} \leftarrow \mathrm{d}_{xy}$ (ν_1), $\mathrm{d}_{x^2-y^2} \leftarrow \mathrm{d}_{z^2}$ (ν_2), and $\mathrm{d}_{x^2-y^2} \rightarrow \mathrm{d}_{xz}\mathrm{d}_{yz}$ (ν_3), respectively, on the basis of distorted octahedral environment around copper. The spectrum of Cu(acac)(bac) exhibits a broad envelope consisting of a band at ~18,350 cm^{-1}, accompanied by a shoulder at ~15,390 cm^{-1}, encompassing more than one overlapping transition. From the shape of electronic absorption bands a distorted octahedral geometry could be expected for this complex. The electronic spectrum of Cu(acac)(dbm) exhibits [36–38] bands at 15,500, 18,520, and 24,390 cm^{-1} attributed to the transitions $\mathrm{d}_{z^2} \leftarrow \mathrm{d}_{xz}\mathrm{d}_{yz}$ (ν_1), $\mathrm{d}_{z^2} \leftarrow \mathrm{d}_{x^2-y^2}$ (ν_2) and $\mathrm{d}_{z^2} \leftarrow \mathrm{d}_{xy}$ (ν_3), respectively, on the basis of a distorted octahedral environment around copper.

3.5. *ESR spectra*

X-band frozen chloroform solution spectra of the copper(II) complexes at 77 K provide two sets of absorption bands (figure 1). One exhibits four-line copper hyperfines ($I = 3/2$) corresponding to doublet–doublet transition ($\Delta M_s = 1$), whereas the second set assigned to triplet–triplet transition ($\Delta M_s = 2$) is observed as a very weak signal approximately at half field (~1 600 G) with respect to the first set of four hyperfine lines. These features of the ESR spectra of copper(II) ternary complexes exhibit characteristics of dimers similar to *bis*-binary copper(II) β-diketonates [21, 22]. The spin–spin interaction of the two copper atoms gives rise to a singlet ($S = 0$) and a triplet ($S = 1$) state due to their proximity. The singlet–triplet transition, normally observed at very high field, is not visible in the spectra of our samples probably due to its spin-forbidden nature [39–41].

The copper hyperfine splitting ($I = 3/2$) corresponding to the $\Delta M_s = 1$ transition exhibits a four-line axial spectrum with well resolved parallel and perpendicular features, except for Cu(acac)(dbm), where perpendicular features are not resolved and yield a broad band. It may be expected that the lifetime of an excited state of the perpendicular feature of Cu(acac)(dbm) is very small and consequently, ΔE becomes sufficiently large resulting in the broadening of the hyperfine lines to such an extent that they merge into a single broad band [41].

The trend of g values (table 2) $g_{\parallel} > g_{\perp} > g_e$ (free electron value) in Cu(acac)(bac) and Cu(bac)(dbm) suggests that the unpaired electron is in the B_{1g} ($d_{x^2-y^2}$) molecular orbital of the complex and the local site geometry is tetragonal with axial elongation. Appreciable difference between the $g_{\parallel}$ and $g_{\perp}$ values indicates a high degree of Jahn-Teller distortion around copper(II). However, in the complex Cu(acac)(dbm) the g values follow the trend $g_{\perp} > g_{\parallel} \approx g_e$ (free electron value) indicating that the unpaired electron lies in the A_{1g} (d_{z^2}) molecular orbital of the complex in the ground state [39, 42, 43]. This ground state is only possible when there is an axial compression of the

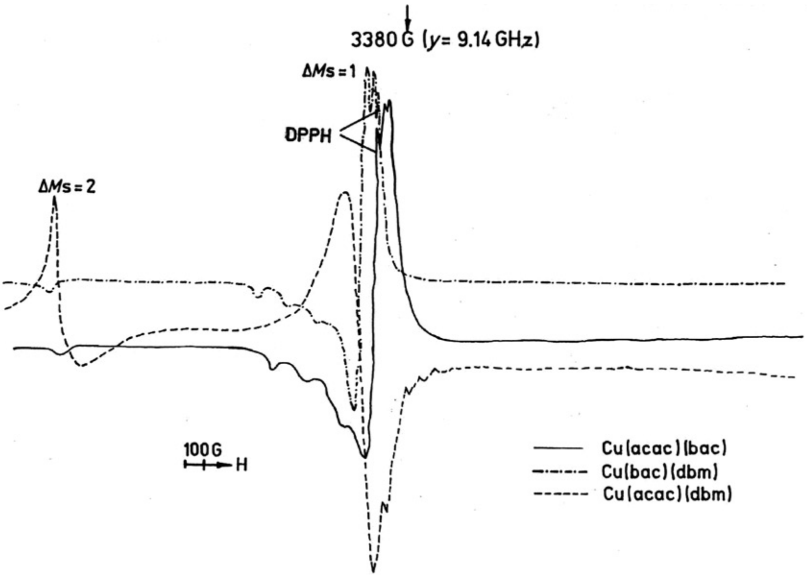

Figure 1. ESR spectra of heterochelate complexes at 77 K.

stereochemistry around the copper(II) ion. It is interesting that there is an axial elongation in Cu(acac)(bac) and Cu(bac)(dbm) and an axial compression in Cu(acac)(dbm).

As the unpaired electron lies in the A_{1g} (d_{z^2}) or B_{1g} ($d_{x^2-y^2}$) orbital, the unpaired electron density in the outer s orbital arises as a result of polarization of inner shell electrons. Further, the extent of unpaired electron density in the s orbital depends on the amount of unpaired electron density present in the d orbital, which polarizes the inner-shell electrons. The outer s orbital unpaired electron spin density ($a_s^2 \times 100$) on copper(II) is proportional to the extent of localization of unpaired electrons on the metal ion [44]. The trend of $a_s^2 \times 100$ values of the copper complexes calculated from the ESR spectra is $Cu(acac)_2 > Cu(acac)(bac) > Cu(bac)(dbm)$. This trend is possible when the unpaired electron of the copper in Cu(bac)(dbm) is more delocalized on the ligands compared to $Cu(acac)_2$ and Cu(acac)(bac). If the mixing coefficients α^2 and β^2 vanish [45], there will be no contribution of the metal orbital to the molecular orbital wave function (φ), i.e. metal–ligand orbital overlap will be zero. In such a case the complexes will be completely ionic and the outer s orbital unpaired electron density would be 100% on the metal ion or equivalent to a free metal ion. As the values of the mixing coefficients increase (or the contribution of the metal orbital to the molecular orbital increases) as a consequence of metal–ligand orbital overlap, the probability of exchange of unpaired electrons onto the ligands increases. Thus, greater metal–ligand orbital overlap, greater will be the exchange of unpaired electrons from metal to ligands. Thus, the lowering in the outer s orbital unpaired electron density indicates a finite value of the mixing coefficient (α^2 and β^2) and the lowering in the a_s^2 value in different complexes will be proportional to the extent of delocalization of unpaired electrons on the ligands, i.e. electron accepting capabilities of the ligands which could be arranged in the following order on the basis of a_s^2 values, $dbm^- > bac^- > acac^-$.

The C_3 carbon of $acac^-$ is expected to be more electron-deficient in Cu(acac)(dbm) as compared to Cu(acac)(bac). Thus, one may expect that the donor capacity of the C_3 carbon of $acac^-$ should be reduced in Cu(acac)(dbm) resulting in axial elongation, but the ESR spectral interpretation provides the reverse result, i.e. stronger bonding capacity of the C_3 carbon of $acac^-$ in Cu(acac)(dbm). Since the β-diketonate ring of $acac^-$ is expected to become more electron deficient in Cu(acac)(dbm) than Cu(acac)(bac) due to ligand to ligand charge transfer through the metal ion, it may be expected that the $acac^-$ of Cu(acac)(dbm) will be more prone to back bonding from copper(II) to the $acac^-$ ($M \rightarrow L$ charge transfer). Thus, a partial double bond character may arise between copper and C_3 carbon of $acac^-$ leading to enhanced bonding in the axial direction. Consequently, an axially compressed stereochemistry may result around the copper(II), consistent with our finding.

Table 2. ESR spectal data of the copper(II) complexes.

	$\Delta M_s = 1$ Transition							$\Delta M_s = 2$ Transition	
Complex	A_{av} (Gauss)	$A_{\parallel}$ (Gauss)	$A_{\perp}$ (Gauss)	g_{av}	$g_{\parallel}$	$g_{\perp}$	$a_s^2 \times 100$	g	H (Gauss)
Cu(acac)(bac)	77.22	185	23.33	2.069	2.195	2.006	4.38	4.02	1625
Cu(bac)(dbm)	73.33	170	25.00	2.103	2.248	2.031	4.16	4.107	1590
Cu(acac)(dbm)		90		2.082	2.006	2.120		4.06	1605

Table 3. Selected positive ion FAB mass spectral data observed from FAB mass spectra of the copper(II) mixed ligand complexes.

	FAB ions (*m*/*z*, % abundance observed)		
Complex	$[m]^+$	$[m+2]^+$	$[m+4]^+$
Cu(acac)(bac)	$\{2M+H]^+$ (647, 5.33)	(649, 4.0)	(651, 4.66)
	$\{M+Cu(bac)(OCCH_2CCH]^+ +$ $[M+(2NBA\text{–}O)+H]^+$ (614, 48.0)	(616, 30.0)	(618, 4.0)
	$\{M+Cu(bac)(OCCH_2CCH+H]^+ +$ $[M+(2NBA\text{–}O)+2H]^+$ (615, 28.0)	(617, 16.0)	(618, 3.5)
	$[M+Cu(CH_3COCHCHO)+$ $(NBA-O)+H]^+$ (609, 36.0)	(611, 34.0)	(613, 12.0)
	$[M+Cu(CH_3COCHCHO)+$ $(NBA-O)+2H]^+$ (610, 16.0)	(612, 12.0)	(614, 48.0)
	$[M+Cu(bac)]^+$ (547, 12.0)	(549, 15.0)	(551, 5.5)
	$[M+Cu(bac)+H]^+$ (548, 6.5)	(550, 5.5)	(552, 10.0)
	$[Cu(bac)_2]^+$ (385, 26.0)	(387, 30.0)	–
	$[Cu(bac)_2+H]^+$ (386, 70.0)	(388, 38.0)	–
	$[Cu(bac)+NBA]^+$ (377, 18.0)	(379, 9.0)	–
	$[Cu(bac)+NBA+H]^+$ (378, 7.5)	(380, 4.0)	–
	$[Cu(acac)(bac)]^+$ (323, 9.5)	(325, 10.0)	–
	$[Cu(acac)(bac)+H]^+$ (324, 30.0)	(326, 14.0)	–
	$[Cu(bac)-H]^+$ (223, 9.0)	(225, 72.0)	–
	$[Cu(bac)]^+$ (224, 38.0)	(226, 25.0)	–
	$[Cu(bac)+H]^+$ (225, 72.0)	(227, 32.0)	–
	$[bac]^+ + [Cu(acac)-H]^+$ (161, 19.0)	(163, 28.0)	–
	$[Cu(acac)]^+$ (162, 8.0)	(164, 6.0)	–
	$[Cu(acac)+H]^+$ (163, 28.0)	(165, 14.0)	–
Cu(acac)(dbm)	$[2M+H]^+$ (771, 1.0)	(773, 2.0)	(775, 1.0)
	$[M+Cu(dbm)(CH_3)+H]^+$ (687, 2.83)	(689, 2.00)	(691, 2.00)
	$[M+Cu(acac)_2+H]^+$ (647, 2.67)	(649, 2.33)	(651, 1.67)
	$[M+Cu(acac)_2+2H]^+$ (648, 2.0)	(650, 1.33)	(652, 1.0)
	$[M+Cu(OH)(C_6H_5)+H]^+$ (543, 4.33)	(545, 3.17)	(547, 3.33)
	$[M+Cu(OH)(C_6H_5)+2H]^+$ (544, 5.33)	(546, 3.0)	(548, 2.0)
	$[M+Cu(C_6H_5)+H]^+$ (526, 3.66)	(528, 3.66)	(530, 2.33)
	$[M+Cu(C_6H_5)+2H]^+$ (527, 5.33)	(529, 2.0)	(531, 1.66)
	$[M+NBA]^+$ (538, 4.66)	(540, 2.33)	–
	$[M+NBA+H]^+$ (539, 2.33)	(541, 2.0)	–
	$[M]^+$ (385, 4.0)	(387, 2.0)	–
	$[M+H]^+$ (386, 2.0)	(388, 1.0)	–
Cu(bac)(dbm)	$[2M+H]^+$ (895, 7.33)	(897, 5.67)	(899, 4.0)
	$[2M+2H]^+$ (896, 7.33)	(898, 2.67)	(900, 6.0)
	$[M+Cu(dbm)]^+$ (733, 9.0)	(735, 7.0)	(737, 6.0)
	$[M+Cu(bac)(OCCH_2CC)]^+$ (737, 6.0)	(739, 6.0)	(741, 3.0)
	$[M+Cu(bac)]^+$ (671, 16.0)	(673, 19.0)	(675, 7.0)
	$[M+Cu(bac)+H]^+$ (672, 11.0)	(674, 7.0)	(676, 11.0)
	$[M+Cu(bac)+2H]^+$ (673, 19.0)	(675, 7.0)	(677, 9.0)
	$[M+Cu(OH)(CH_3COCHCHO)+H]^+ +$ $[Cu(dbm)_2+Cu(OCCH)]^+$ (613, 5.0)	(615, 11.0)	(617, 6.0)
	$[M+Cu(OH)(CH_3COCHCHO)+2H]^+ +$ $[Cu(dbm)_2+Cu(OCCH)]^+$ (614, 20.0)	(616, 16.0)	(618, 6.0)
	$[Cu(bac)_2+Cu(bac)]^+$ (609, 8.0)	(611, 8.5)	(613, 5.0)
	$[Cu(bac)_2+Cu(bac)+H]^+$ (610, 4.50)	(612, 4.5)	(614, 20.0)
	$[Cu(dbm)_2]^+$ (509, 5.0)	(511, 10.0)	–
	$[Cu(dbm)_2+H]^+$ (510, 14.0)	(512, 8.0)	–
	$[Cu(dbm)_2+2H]^+$ (511, 10.0)	(513, 4.0)	–
	$[Cu(bac)(dbm)]^+$ (447, 14.0)	(449, 16.0)	–
	$[Cu(bac)(dbm)+H]^+$ (448, 38.0)	(450, 18.0)	–
	$[Cu(bac)_2]^+$ (385, 22.0)	(387, 24.0)	–

(*Continued*)

Table 3. Continued.

Complex	FAB ions (m/z, % abundance observed)		
	$[m]^+$	$[m+2]^+$	$[m+4]^+$
	$[Cu(bac)_2 + H]^+$ (386, 51.0)	(388, 26.0)	–
	$[Cu(dbm)(C_6H_5) + H]^+$ (364, 7.5)	(366, 4.0)	–
	$[Cu(bac)(C_6H_5) + H]^+$ (302, 22.0)	(304, 11.0)	–
	$[Cu(dbm)]^+$ (286, 4.0)	(288, 3.0)	–
	$[Cu(dbm) + H]^+$ (287, 8.0)	(289, 14.0)	–
	$[Cu(bac)]^+$ (224, 10.0)	(226, 6.0)	–
	$[Cu(bac) + H]^+$ (225, 16.0)	(227, 7.0)	–

NBA = m-Nitrobenzyl alcohol.

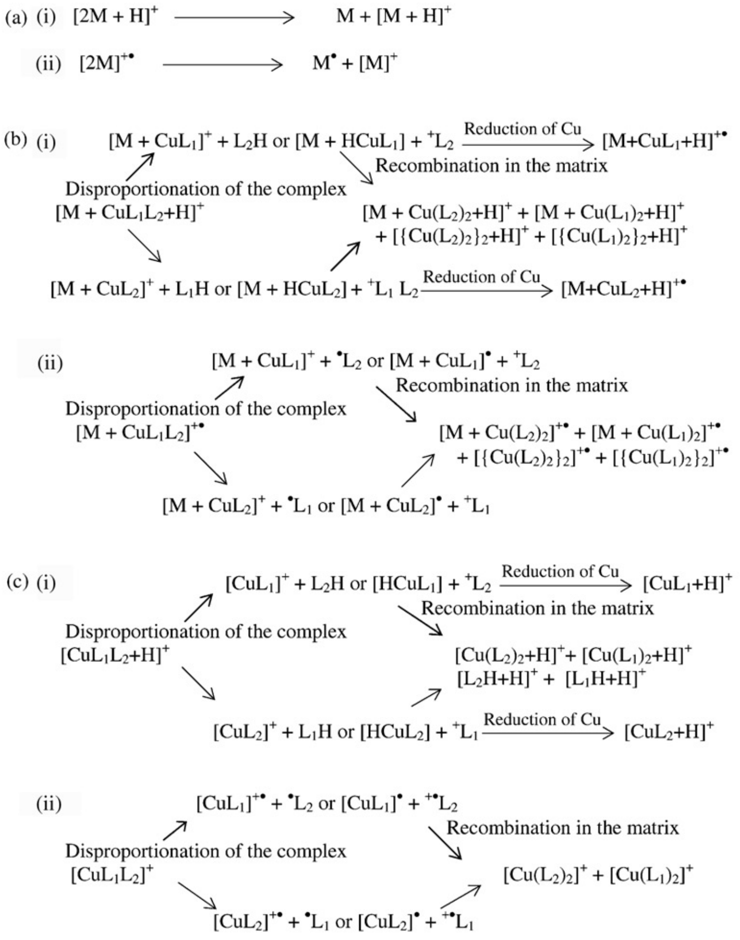

where M = Cu(acac)(bac), Cu(acac)(dbm), or Cu(bac)(dbm); L_1 and L_2 = $acac^{-1}$, bac^{-1} or dbm^{-1}

Figure 2. Fragmentation pattern.

3.6. *Mass spectra*

Most mass spectral reports on copper(II) β-diketonates have been explained without considering isotope distribution [23–26]. The natural abundances of ^{63}Cu and ^{65}Cu are 69.1% and 30.9%, respectively. Therefore, mass spectral peaks of copper complexes and fragment ions having at least one copper atom must exhibit isotope distribution pattern in the abundance ratio $\sim 2:1$. Parent molecular/fragment ion peak containing a ^{63}Cu isotope has been designated as $[m]^+$ ion and peak contributed by a ^{65}Cu isotope has been designated as $[m+2]^+$ ion in the text. Similarly, complex/fragment ion containing two copper atoms in the mass spectrum is expected to exhibit three peaks in the abundance ratios of $\sim 10:9:2$ designated as $[m]^+$, $[m+2]^+$, and $[m+4]^+$, respectively. All the mass spectral peaks of the complexes under the present study exhibiting isotope distribution patterns have been interpreted to arise from molecular/fragment ions containing copper. Those peaks which do not exhibit isotope distribution pattern corresponding to the copper isotopes have been interpreted to arise from either ligands or matrix or their combination.

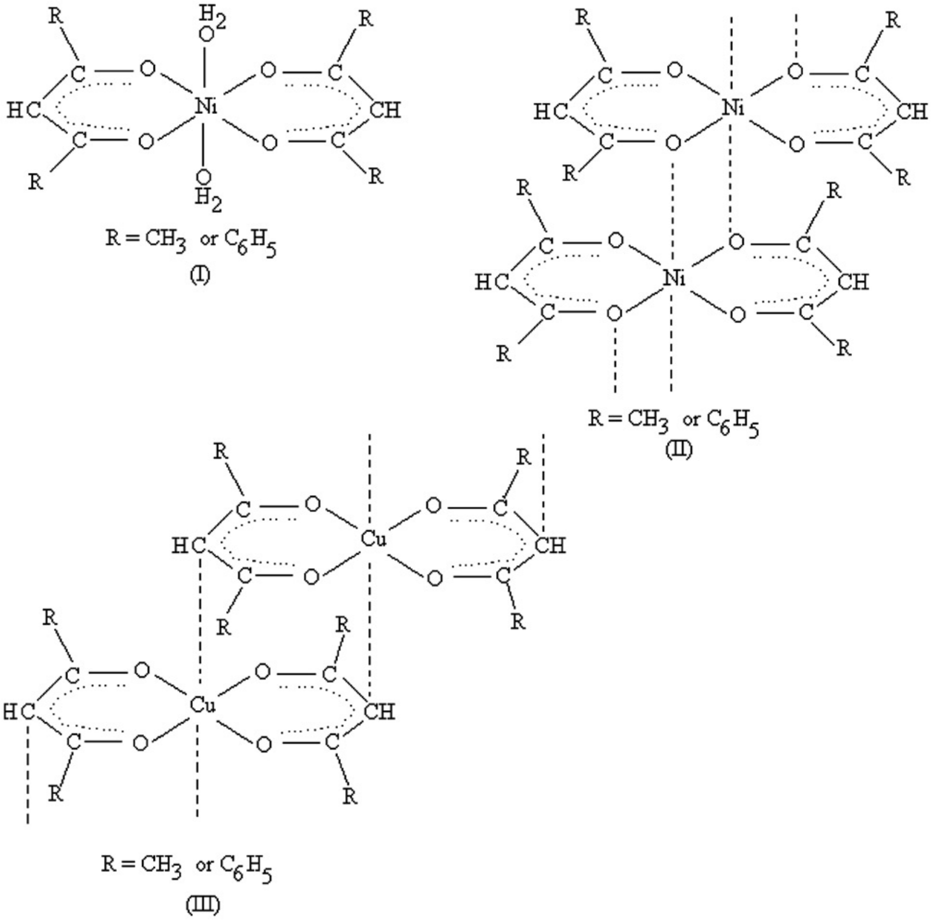

Figure 3. Structures of heterochelate complexes.

FAB mass spectra of the ternary complexes under the present investigation are dominated by the ions derived from the pseudo monomer $[M+H]^+$, pseudo dimer $[2M+H]^+$, matrix *m*-nitrobenzyl alcohol (NBA) and their fragments, in addition to their molecular and dimer ion peaks. Intensities of dimer and their fragment peaks are smaller than those of monomer analogs. Abundances of molecular ion $[M]^+$ and dimer ion $[2M]^+$ peaks are smaller than their respective pseudo molecular ion $[M+H]^+$ and pseudo dimeric ion $[2M+H]^+$ peaks. Presence of mass spectral peaks (table 3) corresponding to the $[2M]^+$, $[2M+H]^+$, $[2M+2]^+$, $[2M+H+2]^+$, $[2M+4]^+$, $[2M+H+4]^+$, $[M+Cu(acac)]^+$, $[M+Cu(bac)]^+$, and $[M+Cu(dbm)]^+$ ions in the spectra of the ternary complexes Cu(acac)(bac), Cu(bac)(dbm), and Cu(acac)(dbm) indicates existence of dimers of the three complexes (figure 2a and 2b). Presence of the ions $[M+Cu(acac)_2+H]^+$, $[M+Cu(bac)_2+H]^+$, and $[M+Cu(dbm)_2+H]^+$ in the FAB mass spectra of the ternary complexes under the present study indicates that the ternary complexes undergo scrambling [23, 24] followed by recombination in the matrix under conditions of the FAB mass spectrometer as shown in the fragmentation scheme (figure 2b). Similarly, presence of peaks corresponding to $[Cu(acac)_2]^+$, $[Cu(bac)_2]^+$, $[Cu(dbm)_2]^+$, $[Cu(acac)_2+H]^+$, $[Cu(bac)_2+H]^+$, and $[Cu(dbm)_2+H]^+$ in the mass spectra of the complexes support the fragmentation scheme (figure 2c). Appearance of the fragment ions $[M+Cu(acac)+H]^+$, $[M+Cu(bac)+H]^+$, $[M+Cu(dbm)+H]^+$, $[Cu(acac)+H]^+$, $[Cu(bac)+H]^+$, and $[Cu(dbm)+H]^+$ in the FAB mass spectrum of the ternary complexes indicates reduction of one of the two copper metal centers of the parent ions (Cu(II) → Cu(I)) in the matrix [23, 24]. Detailed discussion of the FAB mass ions of the Cu(acac)(bac), Cu(acac)(dbm), and Cu(bac)(dam) complexes are described in "Supplementary material".

Complex/fragment ions containing three copper atoms are expected to exhibit four peaks due to isotope distribution of ^{63}Cu and ^{65}Cu in the abundance ratios 10 : 13.5 : 6 : 1 for the $[M]^+$, $[M+2]^+$, $[M+4]^+$, and $[M+6]^+$ ions, respectively. Peaks corresponding to trimeric molecular ions and their fragments are not observed in the mass spectra of Cu(acac)(bac), Cu(acac)(dbm), and Cu(acac)(dbm). Thus, it may be concluded that the complexes Cu(acac)(bac), Cu(acac)(dbm), and Cu(bac)(dbm) are not trimers and possible structures are shown in figure 3.

Supplementary material

Discussion of mass spectra and original FAB mass spectra of the copper complexes can be found in the online version of this article.

Acknowledgements

The authors are thankful to the Head, Department of Chemistry, Banaras Hindu University, for providing laboratory facilities. Thanks are also due to Regional Sophisticated Instrumentation Centre, IIT Chennai, and Regional Sophisticated Instrumentation Centre, Central Drug Research Institute, Lucknow, for recording the ESR and FAB mass spectra, respectively. Mr. V.N. Panday is gratefully acknowledged for recording the IR and electronic spectra. UGC is gratefully acknowledged for providing the financial assistance.

References

[1] E. Meléndez. *Critical Revs. Oncol./Hemato.*, **42**, 309 (2002).
[2] M. Bühl, H.T. Mauschik. *J. Organomet. Chem.*, **648**, 126 (2002).
[3] L.K. Johnson, S. Mecking, M. Brookhart. *J. Am. Chem. Soc.*, **118**, 267 (1996).
[4] G.J.P. Britovsck, V.C. Gibson, B.S. Kimberley, P.J. Maddox, S.J. McTavish, G.A. Solan, A.J.P. White, D.J. Williams. *Chem. Commun.*, 849 (1998).
[5] K. Endo, Y. Moriyasu, S. Misawa, H. Yamasaki, S. Yoshida. *Thin Solid Films*, **206**, 125 (1991).
[6] M.B. Naik, W.N. Gill, R.H. Wentorf, R.R. Reeves. *Thin Solid Films*, **262**, 60 (1995).
[7] B. Zheng, C. Goldberg, E.T. Eisenbraun, J. Liu, A.E. Kaloyeros, P.J. Toscano, S.P. Murarka, J.F. Loan, J. Sullivan. *Mater. Chem. Phys.*, **41**, 173 (1995).
[8] P. Doppelt. *Coord. Chem. Rev.*, **178–180**, 1785 (1998).
[9] Yu.N. Nizel'skii, S.S. Ishchenko, T.E. Lipatova. *Poly. Sci. USSR*, **21**, 700 (1979).
[10] D.P. Graddon. *Coord. Chem. Rev.*, **4**, 1 (1969).
[11] D.A. Thornton. *Coord. Chem. Rev.*, **104**, 173 (1990).
[12] M.F. Farona, D.C. Perry, H.A. Kuska. *Inorg. Chem.*, **7**, 2415 (1968).
[13] R.L. Prasad, R. Bala, R.C. Aggarwal. *Trans. Met. Chem.*, **15**, 379 (1990).
[14] I.A. Baidina, S.A.J. Gromilov. *Struct. Chem.*, **32**, 395 (1991).
[15] Y. Elerman, H. Kara, S. Ozcan, E. Kendi. *Acta Crystallogr., Sect. C*, **56**, 950 (2000).
[16] D.D. Perrin, I.G. Sayce, V.S. Sharma. *J. Chem. Soc. A*, 1755 (1967).
[17] D.R. William. *The Metal Ions of Life*, Van Nostrand Reinhold, London (1971).
[18] N.L. Holy, R.J. Shalvoy. *Org. Chem.*, **45**, 1418 (1980).
[19] C.H. Langford, H.B. Gray. *Ligand Substitution Processes*, W.A. Benjamin, Inc, New York (1967).
[20] M. Anbar. *Mechanism of Inorganic Reactions*, ACS, Advances in Chemistry Series, No. 49, p. 131 (1965).
[21] M. Chikira, T. Isobe. *Chem. Phys. Lett.*, **30**, 498 (1974).
[22] M. Chikira, H. Yokai. *J. Chem. Soc., Dalton Trans.*, 2344 (1977).
[23] (a) C.G. Macdonald, J.S. Shannon. *Aust. J. Chem.*, **19**, 1545 (1966); (b) C.G. Macdonald, J.S. Shannon. *Org. Mass Spectrom.*, **6**, 931 (1972).
[24] J.M. Miller. *Adv. Inorg. Chem. Radio. Chem.*, **28**, 1 (1984).
[25] (a) A.L. Clobes, M.L. Morris, R.D. Koob. *Org. Mass Spectrom.*, **3**, 1255 (1970); (b) A.L. Clobes, M.L. Morris, R.D. Koob. *Org. Mass Spectrom.*, **5**, 633 (1971).
[26] (a) M.L.J. Reimer, J.B. Westmore, M. Das. *Can. J. Chem.*, **70**, 952 (1992); (b) M.L.J. Reimer, J.B. Westmore, M. Das. *Can. J. Chem.*, **71**, 1450 (1993); (c) M.L.J. Reimer, J.B. Westmore, M. Das. *Can. J. Chem.*, **72**, 1302 (1994).
[27] B. Zheng, C. Goldberg, E.T. Eisenbraun, J. Liu, A.E. Kaloyeros, P.J. Toscano, S.P. Murarka, J.F. Loan, J. Sullivan. *Mater. Chem. Phys.*, **41**, 173 (1995).
[28] W.C. Fernelius, B.E. Bryant. *Inorg. Synth.*, **5**, 105 (1957).
[29] P.K. Hon, C.E. Pfluger, R.L. Belford. *Inorg. Chem.*, **5**, 516 (1966).
[30] R.L. Prasad, A. Kushwaha, S.M. Kumar, R.A. Yadav. *Spectrochim. Acta, A*, **69**, 304 (2008).
[31] W.J. Geary. *Coord. Chem. Rev.*, **7**, 81 (1971).
[32] C. Engeltor, D.A. Thornton. *J. Mol. Struct.*, **39**, 25 (1977).
[33] K. Nakamoto. *Infrared and Raman Spectra of Inorganic and Coordination Compounds*, 5th Edn, John Wiley and Sons, Inc, New York (1997).
[34] L. David, C. Craciun, O. Cozar, V. Chis, C. Agut, D. Rusu, M. Rusu. *J. Mol. Struct.*, **563–564**, 573 (2001).
[35] B.N. Figgis, J. Lewis. *Prog. Inorg. Chem.*, **6**, 37 (1964).
[36] F.A. Cotton, G. Wilkinson, C.A. Murillo, M. Bochmann. *Advanced Inorganic Chemistry*, 6th Edn, p. 714, John Wiley & Sons, Inc, New York (1999).
[37] A.B.P. Lever. *Inorganic Electronic Spectroscopy*, p. 376, Elsevier, Amsterdam (1986).
[38] Y. Nishida, S. Kida. *Coord. Chem. Rev.*, **27**, 275 (1979).
[39] D.M. Duggan, D.N. Hendrickson. *Inorg. Chem.*, **13**, 2929 (1974).
[40] T.D. Smith, J.R. Pilbrow. *Coord. Chem. Rev.*, **13**, 173 (1974).
[41] B.A. Goodman, J.B. Raynor. *Inorg. Chem. Radio. Chem.*, **13**, 135 (1970).
[42] G.F. Kokoszka, J. Baranowski, C. Goldstein, J. Orsini, A.D. Mighell, V.L. Himes, A.R. Siedle. *J. Am. Chem. Soc.*, **105**, 5627 (1983).
[43] I. Bertini, D. Gatteschi, A. Scozzafava. *Coord. Chem. Rev.*, **29**, 67 (1979).
[44] M. Symons. *Chemical and Biochemical Aspects of Electron Spin Resonance Spectroscopy*, Van Nostrand Reinhold, London (1978).
[45] H.B. Gray. *J. Chem. Educ.*, **4**, 2 (1964).